# BCL6B-dependent Suppression of ETV2 Hampers Endothelial Cell Differentiation

**Zhonghao Li**

Egbert_hao@126.com

The Third Affiliated Hospital of Guangzhou Medical University

**Wei Wu**

Southern Medical University

**Qiushi Li**

The Third Affiliated Hospital of Guangzhou Medical University

**Xin Heng**

Southern Medical University

**Wei Zhang**

The Third Affiliated Hospital of Guangzhou Medical University

**Yinghong Zhu**

The Third Affiliated Hospital of Guangzhou Medical University

**Lin Chen**

The Third Affiliated Hospital of Guangzhou Medical University

**Ziqi Chen**

The Third Affiliated Hospital of Guangzhou Medical University

**Mengcheng Shen**

Stanford University School of Medicine

**Ning Ma**

Guangzhou national laboratory

**Qingzhong Xiao**

Queen Mary University of London William Harvey Research Institute

**Yi Yan**

The Third Affiliated Hospital of Guangzhou Medical University https://orcid.org/0000-0002-8527-390X

---

**Research Article**

**Keywords:** B-cell CLL/lymphoma 6 member B, Human induced pluripotent stem cell, Endothelial cell, Vessel organoids, ETS variant transcription factor 2

**Posted Date:** February 28th, 2024

**DOI:** https://doi.org/10.21203/rs.3.rs-3968155/v1

## Abstract

# Background

B-cell CLL/lymphoma 6 member B (BCL6B) operates as a sequence-specific transcriptional repressor within the nucleus, playing crucial roles in various biological functions, including tumor suppression, immune response, stem cell self-renew, and vascular angiogenesis. However, whether BCL6B is involved in endothelial cell (EC) development has remained largely unknown. ETS variant transcription factor 2 (ETV2) is well known to facilitate EC differentiation. This study aims to determine the important role of BCL6B in EC differentiation and its potential mechanisms.

# Methods

Doxycycline-inducible human induced pluripotent stem cell (hiPSC) lines with BCL6B overexpression or BCL6B knockdown was established and subjected to differentiate into ECs and vessel organoids (VOs). Quantitative real-time PCR (qRT-PCR) was used to detect the expression of pluripotency and vascular-specific marker genes expression. EC differentiation efficiency was determined by Flow cytometry analysis. The performance of EC was evaluated by *in vitro* Tube formation assay. The protein expression and the vessel-like structures were assessed using immunofluorescence analysis or western blot. Finally, the transcriptional activity of ETV2 was identified by luciferase reporter gene assay.

# Results

Generation of ECs and VOs from hiPSCs. Notably, overexpression of BCL6B suppressed while knockdown of BCL6B improved EC differentiation from hiPSCs. Additionally, the overexpression of BCL6B attenuated the capacity of derived hiPSC-ECs to form a tubular structure. Furthermore, compared to the control VOs, BCL6B overexpression repressed the growth of VOs, whereas BCL6B knockdown had little effect on the size of VOs. Subsequent experiments confirmed the inhibitory effect of BCL6B is facilitated by the binding of BCL6B to the promoter region of ETV2, led to the suppression of ETV2's transcriptional activity.

# Conclusions

BCL6B inhibits EC differentiation and hinders VO development by repressing the transcriptional activity of ETV2.

## Background

B-cell CLL/lymphoma 6 member B (BCL6B), also referred to as BAZF, ZNF62 and ZBTB28, belongs to the B-cell lymphoma 6 (BCL6) gene family [1]. Members of this family encode zinc finger proteins with the Broad-Complex, Tramtrack and Bric a brac/POxvirus and Zinc finger (BTB/POZ) domain, functioning as

sequence-specific transcriptional repressors. The zinc finger motifs and BTB/POZ domain of BCL6B are 94% and 65% identical to those of BCL6 at the amino acid level [1]. Although binding to similar target DNA sequences to act as transcriptional repressors, the tissue expression pattern and pathological function of BCL6B differ from that of BCL6. Some studies have indicated that BCL6B is involved in diverse biological functions, such as facilitating spermatogonial stem cell self-renewal [2], stimulating secondary response of memory CD8 + T lymphocytes [3], and repressing hepatocellular carcinoma [4, 5], colorectal carcinoma [6, 7], and breast cancer [8]. A recent study by Miruto Tanaka et al. showed that BCL6B contributes to ocular vascular diseases via Notch signal silencing [9]. BCL6B is enriched in endothelial cells (ECs) [10], however, as a transcriptional repressor, the function and mechanisms through which BCL6B regulates EC development remain poorly understood.

Human induced pluripotent stem cells (hiPSCs) have the capability to differentiate into various cell types [11]. This property holds great promise for studying human development, cell differentiation and the role of critical transcriptional factors in cell fate decision [12]. Recent advances in hiPSC-derived organoid enable a better recapitulation of the three dimensional (3D) microstructures and functions of human tissues [13]. This progress provides a more sophisticated tool for exploring human development and cell differentiation [14].

In this study, utilizing both hiPSC-derived 2D ECs and 3D vessel organoids (VOs), we uncovered that BCL6B hampers EC differentiation and VO development by repressing the transcriptional activity of ETV2.

## Methods

# hiPSC culture and EC differentiation

hiPSCs (passage 25–40) were maintained under feeder-free conditions in defined E8 media (Gibco, A1516901) on tissue culture plates coated with hESC-qualified Matrigel (Corning, 354277) at 37°C in 5% CO2. The culture medium was exchanged daily. Routine passaging of hiPSCs at 1:4, and single-cell dissociation were carried out using Accutase solution (Sigma, A6964). The hiPSCs were cryopreservation with CryStor CS10 (Stemcell, 100–1061). In addition, we performed a mycoplasma contamination test every two weeks to ensure the health of all the cell lines (data not shown).

The EC differentiation protocol was adapted from a published protocol [15]. In brief, hiPSCs were cultured in Essential 8 medium reached ~ 80% confluency, then were dissociated into single cells, and seeded in 6-well plates with 10 μM ROCK inhibitor Y27632 (Selleck, S1049) on D0 at a density of $10^5$ cells/well. On D1, hiPSCs were treated with 8 μM CHIR99021 (Selleck, S2924) in Chemically Defined Medium (CDM) for 3 days. On D4, differentiated cells were treated with 50 ng/ml VEGF (PeproTech, 100 − 20) and 10 mM SB431542 (Selleck, S1067) until cells reached ~ 100% confluent on D6. For cell dissociation, TrypLE Select Enzyme (10×) (Gibco, A1217701) was used for 10 min until most cells became singlets. The cells were then passed through a 40-μm strainer. Cell dissociation was neutralized by adding 2 ml of Endothelial Cell Medium (ECM, ScienCell, 1001), followed by magnetic associated cell sorting (MACS) to

purify hiPSC-derived ECs with CD144 (VE-Cadherin) MicroBeads (Miltenyi, 130-097-857) or subjected to flow cytometry analysis. The CDM consists of IMDM(50%); Ham's F12 Nutrient Mix (50%); BSA (0.25%); Lipid concentrate (1X); ITS (0.1%); Ascorbic acid (50 μg/ml); Monothioglycerol (450 μM); and Glutamax (1X).

# Generation of human blood VOs

A step-by-step protocol detailing the differentiation of the human VOs can be found in Nature Protocol [16]. Briefly, hiPSCs were dissociated into single cells with Accutase. Subsequently, the cells were resuspended in the E8 medium containing 10 μM Y27632 and seeded at 1,000 cells/well in round bottom ultra-low attachment 96-well plates (Costar, 7007) on D − 1, with a volume of 100 μl per well. The plate was then centrifuged at 100 g for 3 min to assemble hiPSCs into embryoid bodies (EBs) and placed in an incubator at 37°C with 5% CO2. After 24 h (D0), the culture medium was replaced by the N2B27 medium with 12 μM CHIR99021 and 30 ng/ml BMP4 (PeproTech, 120-05). On D3, the N2B27 medium was renewed with 100 ng/ml VEGF and 2 μM forskolin (HY-15371). Starting from D6, the resulting cell aggregates were embedded in Matrigel:Collagen I (1:1) gels and overlaid with ECM containing 15% FBS, 100 ng/mL VEGF and 100ng/ml FGF-2 (PeproTech, 100-18B). This medium was changed every two days. Around D10-12 vascular networks were established, and either directly analyzed or networks from individual cell aggregates were extracted from gels and further cultured in round bottom ultra-low attachment 96-well plates. These vascular networks self-assembled into vascular organoids, and the medium was changed every three days until organoids were ready for analysis.

# Establishment of BCL6B overexpression and knockdown hiPSC lines

The human BCL6B coding regions, fused with Flag tags, was amplified through polymerase chain reaction (PCR) using hiPSC cDNA as template. Subsequently, these templates were cloned into adapted FUW-tetO-MCS vector (MiaoLingBio, P48786). Concurently, shRNA constructs were generated using the Tet-pLKO-puro vector (MiaoLingBio, P0171), following previously described methods [17]. For viral production, 10 μg of target vectors (BCL6B-FLAG, BCL6B shRNA, and FUW-M2rtTA (MiaoLingBio, P0521), along with lentiviral envelope and the packaging plasmids psPAX2 (MiaoLingBio, P0261) and pMD2.G (MiaoLingBio, P0262), were transfected into 293T cells using lipofectamine 3000 (Invitrogen, L3000015). After 72 hours, lentivirus supernatants were collected and filtered through a 0.45 μm syringe filter. hiPSCs were coinfected with BCL6B-FLAG and FUW-M2rtTA or infected solely with BCL6B shRNA lentivirus using a spin infection method, as previously described [18]. Two days post-infection, puromycin-resistant clones positive clones were selected using 1 μg/ml puromycin (MCE, HY-B1743A) for 4 days to establish BCL6B overexpression (BCL6B OE) or BCL6B knockdown (BCL6B KD) hiPSC lines, respectively. The successful establishment of hiPSC lines was confirmed by western blotting and then applied for later differentiation.

# Immunofluorescence analysis

For hiPSCs-derived ECs, the purified ECs were seeded in a 24-well plate with coverslips and cultured until reaching 100% confluence. The cells were fixed in 4% paraformaldehyde (PFA) for 15 min, permeabilizated with 0.5% Triton X-100 for 10 min, followed by blocking with 10% goat serum for 30 min. Subsequently, the cells were incubated with mouse anti-CD31 (Abcam, ab9498) and rabbit anti-VE Cadherin (ab33168) at 4°C overnight. Secondary antibodies used were Alexa Fluor 488-conjugated goat anti-rabbit (Abcam, ab150077) and Alexa Fluor 647-conjugated goat anti-Mouse (Abcam, ab150115). DAPI (Sigma, D9542) was used to mark cell nuclei. Stained coverslips were mounted with mounting medium and stored at 4°C before imaging. All images were acquired by confocal imaging systems.

For whole-mount staining of organoids, the samples were fixed in 4% PFA for 1 hour at room temperature (RT), followed by three washes with PBS. Subsequently, the organoids were incubated in 0.5% TritonX-100 at RT for 1 hour. After blocking with 5% BSA in 0.1% TritonX-100 at RT for 1 hour, organoids were incubated with primary antibodies at 4°C for 48 hr, washed with PBS, and then incubated with secondary antibodies at 4°C for 48 hr. The stained organoids underwent three washes with PBS before being mounted on glass microscope slides using Mounting Medium (Invitrogen, P36961). To preserve the 3D structure of the organoids before confocal imaging, Polybead Microspheres were placed between the slide and the coverslip.

# Flow cytometry analysis

HiPSC-ECs (D6) were dissociated into single-cell suspensions using TrypLE Select Enzyme for 8–10 min. After resuspension in staining buffer (Biolegend, 420201), approximately $0.5 \times 10^6$ single cells for each group were incubated with PE anti-human CD144 antibody (Biolegend, 348506) and FITC anti-human CD31 antibody (Biolegend, 303104) for 30 min. The results were analyzed using the BD LSR FortessaX-20 cytometer and FlowJo software.

The vascular organoids (D15) were mechanically disrupted and disaggregated using 3U/mL Dispase (Gibco, 17105041), 2U/mL Liberase (Sigma, 5401020001) and 100U DNAse (Stemcell, 07900) in PBS for 30 min at 37°C while rotating. Subsequently, single cells were stained with the following antibodies for 30 min: PE anti-human CD144 antibody (Biolegend, 348506), FITC anti-human CD31 antibody (Biolegend, 303104) and APC anti-human PDGFRβ antibody (Biolegend, 323608), followed by FACS analysis.

# RNA extraction, cDNA synthesis, and qRT-PCR

The total RNA of hiPSCs, hiPSC-ECs and 10 VOs was extracted using Trizol (Invitrogen, 15596026), followed by reverse transcription to generate cDNA using the HiScript II 1st Strand cDNA Synthesis Kit (Vazyme, R212-01). qRT-PCR was performed using the Applied Biosystems QuantStudio 5 qPCR system with the ChamQ SYBR qPCR Master Mix (Low ROX Premixed) (Vazyme, Q331-02). Relative mRNA expression was determined by the delta cycle time with human GAPDH serving as the internal control for data normalization. The primer sequences were as follows:

GAPDH: forward, 5'-TCGGAGTCAACGGATTTGGT-3', reverse, 5'-TTCCCGTTCTCAGCCTTGAC-3';NANOG: forward, 5'-CAATGGTGTGACGCAGAAGG-3', reverse, 5'-TGCACCAGGTCTGAGTGTTC-3';

OCT4: forward, 5'-CTCGAGAAGGATGTGGTCCG-3', reverse, 5'-TGACGGAGACAGGGGGAAAG-3';

PECAM1: forward, 5'-AGACGTGCAGTACACGGAAG-3', reverse, 5'-TTTCCACGGCATCAGGGAC-3';

VE-Cadherin: forward, 5'-CGCAATAGACAAGGACATAACAC-3', reverse, 5'-GGTCAAACTGCCCATACTTG-3';

VWF: forward, 5'-CCCGAAAGGCCAGGTGTA-3', reverse, 5'-AGCAAGCTTCCGGGGACT-3';

VEGFR2: forward, 5'-GAGGGGAACTGAAGACAGGC-3', reverse, 5'-GGCCAAGAGGCTTACCTAGC-3';

PDGFRβ: forward, 5'-ATCAGCAGCAAGGCGAGC-3', reverse, 5'-CAGGTCAGAACGAAGGTGCT-3'.

# Western blotting

Cell pellets were lysed using RIPA buffer containing 1% PMSF. Protein concentration was measure by the BCA method using a Pierce BCA Protein Assay Kit (23225, Thermo Fisher Scientific). Samples were resolved on 10% sodium dodecyl sulfate polyacrylamide gels (SDS-PAGE), followed by transfer to a PVDF membrane at 100v for 120 min. Membranes were blocked with 5% non-fat dry milk in 1xTBST at RT for 1 h and then incubated with primary antibody at 4°C overnight. The following antibodies were used: mouse anti-CD31 (Abcam, ab9498); rabbit anti-VE Cadherin (ab33168); rabbit anti-VWF (ab6994); rabbit anti-BCL6B (Origene, TA369826); rabbit anti-FLAG (Abcam, ab205606); and mouse anti-beta actin (Abcam, ab8226). After appropriate washing with 1xTBST, the membranes were incubated with Goat Anti-Rabbit IgG H&L (HRP) (Abcam, ab6721) or Goat Anti-Mouse IgG H&L (HRP) (Abcam, ab6789) at RT for 1 hr. A chemiluminescent assay was performed using ECL substrates (Abcam, ab133406), and signals were detected with a FUSION Solo S chemiluminescence imaging system (5200 Muti, Tanon)

# Tube formation assay

hiPSC-ECs were seeded onto 96-well plates coated with 50 µl matrigel (BD, 356231) at a density of $2\times10^4$ cells per well and then incubated for 4 hours. Tubular structures were photographed under a light microscope (Zesis) and analyzed using Image J software (NIH, Bethesda, MD).

# Statistical Analysis

Results are presented as mean ± SD from a minimum of three independent experiments. Group comparisons were conducted using the non-paired two-tailed Student's t-test. In cases of non-normal distribution, the two-tailed F test was employed. For comparisons involving more than two groups, ANOVA was applied. A $p$ value of $< 0.05$ were considered statistically significant.

## Results

# Generation and characterization of ECs from hiPSCs

To investigate whether BCL6B plays a functional role in endothelial cell (EC) development, a feeder-free, and chemically defined protocol (Fig. 1A) was adapted in this study to generate ECs from human induced pluripotent stem cells (hiPSCs). Throughout the differentiation process, cell morphology was gradually changed (Fig. 1B). Differentiated hiPSC-derived ECs were purified using a CD144 antibody before being re-plated for further characterization on D7 (Fig. 1C). The purified cells displayed a typical EC morphology (Fig. 1C) and were positive for canonical EC markers, VE-Cadherin and CD31 (Fig. 1C). We further confirmed that hiPSC-derived ECs shared a comparable capillary-like tube formation capacity as human umbilical vein endothelial cells (HUVECs) (Fig. 1D). Quantitative data revealed similar junction number and tube length between HUVECs and hiPSC-derived ECs (Fig. 1E), suggesting functionally similarities between primary and hiPSC-derived ECs.

The differentiation of hiPSCs into ECs involved two stages: mesoderm induction and EC fate specification. Using quantitative real-time PCR (qRT-PCR), we observed a gradual increase in the gene expression levels of *PECAM1*, *CDH5*, *VWF*, and *BCL6B* during the hiPSC-EC differentiation process from D0 to D6. (Fig. 1F). The protein expression of VWF and VE-cadherin exhibited the same increasing pattern as their transcriptional levels throughout the hiPSC differentiation process. Surprisingly, the protein expression levels of BCL6B followed an opposite trend, becoming barely detectable between D5 and D6 of EC differentiation when EC markers peaked (Fig. 1G). This suggests that lower expression of BCL6B at the protein level is required for EC differentiation, whereas high expression of BCL6B at the protein level could affect EC generation.

# BCL6B overexpression suppressed EC differentiation from hiPSCs

To investigate the involvement of BCL6B in EC differentiation, we developed a doxycycline inducible BCL6B-flag expression vector (Fig. 2A), and established an inducible hiPSC line to control the temporal expression of BCL6B upon the addition of doxycycline (Fig. 2B). Next, we treated the inducible hiPSC line with doxycycline to induce BCL6B overexpression throughout the EC differentiation process (Fig. 2C). The differentiation efficiency, assessed by flow cytometry analysis of $CD144^+$ cells on D6, revealed that compared to the differentiation efficiency of control hiPSCs at 8.55% ±0.13%, overexpression of BCL6B in hiPSCs resulted in a decrease in the differentiation of hPSCs into ECs, with efficiencies of 5.54% ± 0.25%. In contrast, the group treated with doxycycline alone displayed no significant differences (Fig. 2, D and E).

Given that the differentiation of EC from hiPSCs involves two stages and mesodermal cells express high levels of BCL6B (Fig. 1G), we further asked if EC differentiation efficiency could be temporally controlled by BCL6B activation. To test this, we treated the inducible hiPSCs with doxycycline at different time points until D6 of EC differentiation (Fig. 2F). Our western blot analysis confirmed that two days of doxycycline treatment were sufficient to achieve high expression levels of BCL6B (Fig. 2G). However, we observed that, regardless of the timing of doxycycline treatment, all groups exhibited decreased EC differentiation, although overexpression of BCL6B initiated in the early stages tended to show more severe inhibitory effects on EC differentiation (Fig. 2, H and I). Furthermore, the overexpression of BCL6B

during differentiation significantly attenuated the capacity of derived hiPSC-ECs to form a tubular structure, suggesting compromised EC function of BCL6B-overexpressing hiPSC-derives ECs (Fig. 2J). The above results clearly show that overexpression of BCL6B inhibits hiPSCs differentiation into ECs.

# Downregulation of BCL6B improved EC differentiation from hiPSCs

To firmly establish a causal role for increased BCL6B activity in reduced EC differentiation efficiency and functional properties, we further investigated whether inhibiting the expression of BCL6B in hiPSCs would enhance their capacity to generate ECs. To achieve this, we constructed doxycycline-inducible vectors for effective silencing of endogenous BCL6B in hiPSCs upon doxycycline treatment (Fig. 3, A and B). Subsequently, we initiated EC differentiation in the presence of doxycycline at six time points (D0, 1, 2, 3, 4, and 5) during the differentiation process (Fig. 3C). Our findings revealed that knockdown of BCL6B significantly increased EC differentiation, with efficiencies increasing from 9.4% ± 0.11–15.8% ± 0.23% (Fig. 3, D and E). Furthermore, the highest differentiation efficiency was observed when BCL6B inhibition was initiated earlier than D1 of differentiation (Fig. 3, D and E), which was consistent with the observation that a more profound inhibitory effect of BCL6B overexpression on EC differentiation was achieved at D0 of differentiation (Fig. 2I). Moreover, knocking down of BCL6B significantly increased the protein expression of VWF, VE-cadherin and CD31 in hiPSC-ECs (Fig. 3F). However, the derived hiPSC-ECs with BCL6B knockdown did not demonstrate enhanced tubular structure formation capacity when compared to those without BCL6B inhibition during the differentiation process (Fig. 3G).

# BCL6B impaired blood vessel organoids generation

To further validate the critical role of BCL6B in vessel development within a more complex context, we generated vessel organoids (VOs) from hiPSCs. Briefly, hiPSCs were assembled into embryoid bodies (EBs) via centrifugation in ultra-low attachment 96-well plates, followed by a 24-h incubation prior to mesoderm induction using CHIR99021 and BMP4 (Fig. 4A). After 3 days, the differentiated EBs were treated with VEGF and forsklin for 2 additional days for further vascular lineage development. Subsequently, the EBs were embedded in Matrigel:Collagen I (1:1) gels to promote EC sprouting and structure maturation. Brightfield imaging of VOs showed a significant increase in the size of VOs throughout the differentiation process (Fig. 4B). Confocal imaging revealed the formation of complex, interconnected vascular networks by $CD31^+$ ECs (Fig. 4C). Moreover, these self-organizing 3D VOs exhibited proper localization of pericytes, defined by the molecular markers -SMA. Additionally, the vessel-like structures were enveloped by a basement membrane, as confirmed by immunostaining for Collagen IV (Col ) (Fig. 4D)

We further performed qRT-PCR to determine the expression of pluripotency and vascular-specific marker genes in VOs. At D15 of differentiation, hiPSC-VOs were negligible for *OCT4*, *NANOG*, and *SOX2*, and showed drastic upregulation of EC markers (*PECAM1*, *CDH5*, *VWF*, *and VEGFR2*) and a pericyte marker (*PDGFRβ*) (Fig. 4E). In line with this, our flow cytometry results revealed that approximately 33.4% of total

cell population in the hiPSC-VOs were $CD144^+$ ECs at D15 of differentiation (Fig. 4F). To determine whether hiPSC-VOs respond to proinflammatory cytokines with a pro-adhesive phenotype, we challenged the hiPSC-VOs with lipopolysaccharides (LPS). Immunofluorescence analysis showed a significant increase in intracellular adhesion molecule-1 (ICAM1) level upon LPS treatment (Fig. 4G). Thus, we have successfully established a fully structured and functional human VO model.

With the successful establishment of blood VOs, we proceeded to generate BCL6B gene-perturbed blood VOs using the previously developed inducible hiPSC lines. Remarkably, the control VOs showed a gradual increase in the size from 219.9 ± 3.5 μm at D0 to 1067.3 ± 24.6 μm at D5 (Fig. 5A). In contrast, BCL6B overexpression, particularly after D2 of differentiation, significantly repressed the growth of VOs (from 212.6 ± 3.8 μm at D0 to 717.3 ± 24.2 μm at D5), whereas BCL6B knockdown had little effect on the size of VOs (from 220.9 ± 4.5 μm at D0 to 1073.4 ± 29.2 μm at D5 ) (Fig. 5, A and B). BCL6B knockdown significantly upregulated the expression levels of *CD31*, *VWF* and *VEGFR2*, while BCL6B overexpression downregulated the expression levels of *VEGFR2* and *PDGFRβ* in D15 hiPSC-VOs (Fig. 5C). Importantly, Immunofluorescence staining showed that both Col IV and PDGFRβ proteins were significantly downregulated upon BCL6B overexpression in day 15 hiPSC-VOs (Fig. 5D). Collectively, these data strongly suggest that BCL6B is a negative regulator in EC differentiation and vascular network formation in hiPSC-derived VOs.

# BCL6B inhibited ETV2 transcription

To identify the potential downstream targets regulated by BCL6B during EC differentiation, we conducted transcriptional analysis on several transcription factors associated with vascular EC differentiation or vascular development [19, 20]. These factors include ETS proto-oncogene 1 (ETS1), ETS proto-oncogene 2 (ETS2), ETS transcription factor ERG, ETS transcription factor ELK3, Fil1, ETS variant transcription factor 2 (ETV2) [21, 22], ETS variant transcription factor 6 (ETV6), and VEGFR2. Among them, the induction of BCL6B overexpression in hiPSCs through doxycycline significantly decreased the mRNA expression of *ETV2* and *VEGFR2* during the EC specification stage (Fig. 6A). Previous study showed that ETV2 activation facilitates EC differentiation from hiPSCs [23]. We found that the abrogation of BCL6B expression significantly enhanced the transcription of ETV2 in the initial 3 days of EC differentiation. (Fig. 6B).

It has been well-known that BCL6B is a transcription repressor. To further investigate whether BCL6B is capable of binding to ETV2 promoter and repress its transcription, we first analyzed the ETV2 promoter using JASPAR website (https://jaspar.elixir.no/), and found that a putative binding site of BCL6B upstream of the ETV2 promoter region between − 1145 bp to -1129 bp. We then generated three different ETV2 promoter-luciferase constructs, one carrying a 2-kb ETV2 promoter (pGL3-ETV2, Fig. 6C), another one carrying a 1.1-kb truncated promoter by deleting the BCL6B binding site (pGL3-ETV2-del, Fig. 6D), and the third one carrying a 2.0 kb promoter but in which the BCL6B binding site is mutated (pGL3-ETV2-mut, Fig. 6E). We next examined the effect of BCL6B on the ETV2 luciferase reporter in 293T cells, and found that BCL6B overexpression dramatically decreased the full-length ETV2 gene promoter activity. In

response to BCL6B overexpression, both constructs carrying either a truncated (pGL3-ETV2-del) or a mutated (pGL3-ETV2-mut) ETV2 gene promoter exhibited a much higher level of promoter activity, compared to pGL3-ETV2 (Fig. 6F). Importantly, a much lower ETV2 gene promoter activity was observed in both the truncated (pGL3-ETV2-del) and the mutated (pGL3-ETV2-mut) ETV2 gene promoter vector in absence of BCL6B overexpression, suggesting that BCL6B binding element within ETV2 gene promoter is important for ETV2 gene transcription at base level. Our results show that BCL6B is able to bind to ETV2 promoter and suppress ETV2 gene expression.

# Discussion

ECs derived from hiPSCs with their unlimited expansion potential, are considered an alternative cell source for experimental studies, and especially, therapeutic approaches [24]. Generally, there are 3 primary methods for EC derived from differentiating embryonic stem cells (ESCs) or iPSCs [25]. First, ESC and iPSC can be differentiated into 3D EBs, in which spontaneously undergo differentiation into the three germ layers: ectoderm, endoderm, and mesoderm, with emergence of numerous lineages of cells. Addition of a variety of growth factors promotes EC differentiation within the EB. In a second method, coculture of differentiating ESC or iPSC with other stromal cells to promote EC lineage differentiation from the mesoderm. Finally, EC differentiation performed in 2D culture on cell culture plates coated with Matrigel or other proteins using specific culture mediums with sequentially added recombinant growth factors. Several independent laboratories have successfully generated ECs from hiPSCs or human pluripotent stem cells (hPSCs). Amy Cochrane. et al. [26] reported that the efficiency of EC differentiation from hiPSCs was 62%. An approximately 15% CD31 + cells was observed in differentiating EBs derived from mouse ESCs [27]. Moreover, about 18%~33% differentiation efficiency was achieved with some hiPSC lines [28–30]. In our study using the adapted protocol, we observed a basal differentiation efficiency of approximately 10%, which was much lower than that (61.8%~88%) in original protocol [15], while Yingyi Quan et al. [31] reported a 43.5% differentiation efficiency in their study when followed the original protocol. Although defined conditions have been described, a very low efficiencies of EC differentiation (< 1.5%) was also observed in the early protocols [32]. Multiple factors, for example, fetal bovine serum (FBS), bovine serum albumin (BSA), the quality and source of stem cell lines, and growth factors, may attribute to the different EC differentiation efficiency reported in various studies.

BCL6B is reported to be involved in a diversity of biological functions, including tumor suppression[4, 6, 8], immune response[3], stem cell self-renew[2], and vascular angiogenesis[10], all of which are related to its function as a transcriptional repressor. Given its role as a transcriptional repressor, we anticipated a broader functional impact with BCL6B. Online database indicated a high mRNA expression level of BCL6B in human ECs [10], which is consistent with our qRT-PCR data. However, at the protein level, the BCL6B expression is notably low. This discrepancy adds intrigue to unveiling its role in EC development and function. We constructed inducible overexpression and knockdown vectors to manipulate BCL6B expression during EC differentiation from hiPSCs and VO generation from hiPSCs. The data clearly demonstrated that BCL6B inhibits EC differentiation. Although we clearly observed that knockdown of BCL6B in hiPSCs significantly increased EC differentiation, impaired BCL6B expression in hiPSC-derived

ECs exhibited negligible effect on tube formation. However, Ohnuki et al. reported that BCL6B knockdown abrogated EC network formation in HUVEC [10], indicating that BCL6B may play a distinct role in primary and hiPSC-derived ECs. Similar to tube formation, we also found that BCL6B overexpression impaired the size of VOs during the first 5 days of differentiation, whereas knockdown of BCL6B had little effect on VO size. Mechanistically, we uncovered that BCL6B inhibits ETV2 transcription, consequently inhibiting EC differentiation. As a transcriptional repressor, BCL6B is expected to have numerous binding sites in the genome, and other potential targets of BCL6B may contribute to the inhibition of EC differentiation from hiPSCs. A comprehensive approach to interrogate the potential targets of BCL6B would involve using ChIP-seq technology. Additionally, the inconsistency between BCL6B mRNA and protein expression during EC differentiation suggests a negative-feedback regulation in BCL6B gene regulation during EC differentiation from hiPSCs, which merit further investigation.

ECs line the interior of all blood and lymphatic vessels, playing key roles in delivering oxygen and nutrients, regulating blood flow, modulating immune cell trafficking and maintaining tissue homeostasis[33]. Vascular EC dysfunction is central to the progression of most chronic conditions, including ischemic heart disease [34] and stroke [35], the top two global causes of mortality. A published study has demonstrated that BCL6B contributes to ocular vascular diseases via notch signal silencing [9].

# Conclusion

In conclusion, this study is the first time to demonstrate that BCL6B can modulate EC differentiation as well as blood VO development. Our study reveals a new role of BCL6B in EC development and function, making it a potential target for vascular diseases.

# Abbreviations

**BCL6B**
B-cell CLL/lymphoma 6 member B
**EC**
Endothelial cell
**ETV2**
ETS variant transcription factor 2
**hiPSC**
Human induced pluripotent stem cell
**VO**
Vessel organoids
**qRT-PCR**
Quantitative real-time PCR
**BCL6**
B-cell lymphoma 6
**BTB/POZ**

Broad-Complex, Tramtrack and Bric a brac/POxvirus and Zinc finger domain

**HUVECs**

Human umbilical vein endothelial cells

**EBs**

Embryoid bodies

**Col Ⅳ**

Collagen IV

**LPS**

lipopolysaccharides

**ICAM1**

Intracellular adhesion molecule-1

**ETS1**

ETS proto-oncogene 1

**ETS2**

ETS proto-oncogene 2

**ETV6**

ETS variant transcription factor 6

**ESCs**

Embryonic stem cells

**hPSCs**

Human pluripotent stem cells

**FBS**

Fetal bovine serum

**BSA**

Bovine serum albumin

# Declarations


### Acknowledgments

The hiPSC line was acquired from Dr. Guangjin Pan’s laboratory at the Guangzhou Institutes of Biomedicine and Health, Chinese Academy of Sciences. This study is supported by grants from the International Cooperation Project of Guangdong Science and Technology (2022A0505050079), the Natural Science Foundation of Guangdong Province (2021A1515011620), the National Natural Science Foundation of China (82200355), the Guangzhou Basic and Applied Basic Research Foundation (2023A04J1204), Science and Technology Projects in Guangzhou (202201020189), and China Postdoctoral Science Foundation (2022M720904).


### Author contributions

Y.Y, Q.X, N.M and W.W conceptualized and supervised the study. Z.L conducted the majority of the experiments, acquired and analyzed data, and wrote the manuscript. N.M contributed to writing and revising the manuscript. Q.L, X.H and W.Z collected and processed the samples. Y.Z, L.C, Z.C and M.S reviewed the manuscript and provided helpful comments. Y.Y, Q.X, N.M and W.W read the manuscript, offered insightful comments, and secured funding. All authors have read and approved the final version of this manuscript.

### Availability of data and materials

All data generated or analysed during this study are included in this published article. Data generated during the current study are available from the corresponding author on reasonable request.

### Ethics approval and consent to participate

Not applicable.

### Consent for publication

Not applicable.

### Competing interests

The authors declare that they have no competing interests.

### Author details

[1]Department of Cardiology, Translational Research Center for Regenerative Medicine and 3D Printing Technologies, Guangdong Provincial Key laboratory of Major Obstetric Diseases; Guangdong Provincial Clinical Research Center for Obstetrics and Gynecology; The Third Affiliated Hospital of Guangzhou Medical University, Guangzhou 510150, China. [2]Department of Pathophysiology, School of Basic Medical Sciences, Southern Medical University, Guangzhou 510515, China. [3]Stanford Cardiovascular Institute, Stanford University School of Medicine, Stanford 94305, USA. [4]Guangzhou National Laboratory, Guangzhou 510005, China

[5]Centre for Clinical Pharmacology, William Harvey Research Institute, Faculty of Medicine and Dentistry, Queen Mary University of London, London E1 4NS, UK. [6]Key Laboratory of Cardiovascular Diseases at The Second Affiliated Hospital of Guangzhou Medical University and Guangzhou Municipal, Guangdong Provincial Key Laboratory of Protein Modification and Degradation, School of Basic Medical Sciences, Guangzhou Medical University, Guangzhou 511436, China.

# References

1. Okabe S, Fukuda T, Ishibashi K, Kojima S, Okada S, Hatano M, Ebara M, Saisho H, Tokuhisa T. BAZF, a novel Bcl6 homolog, functions as a transcriptional repressor. Mol Cell Biol. 1998;18(7):4235–44.
2. Oatley JM, Avarbock MR, Telaranta AI, Fearon DT, Brinster RL. Identifying genes important for spermatogonial stem cell self-renewal and survival. Proc Natl Acad Sci U S A. 2006;103(25):9524–9.
3. Manders PM, Hunter PJ, Telaranta AI, Carr JM, Marshall JL, Carrasco M, Murakami Y, Palmowski MJ, Cerundolo V, Kaech SM, et al. BCL6b mediates the enhanced magnitude of the secondary response of memory CD8 + T lymphocytes. Proc Natl Acad Sci U S A. 2005;102(21):7418–25.
4. Wang W, Huang P, Wu P, Kong R, Xu J, Zhang L, Yang Q, Xie Q, Zhang L, Zhou X, et al. BCL6B expression in hepatocellular carcinoma and its efficacy in the inhibition of liver damage and fibrogenesis. Oncotarget. 2015;6(24):20252–65.
5. Li X, Guo M, Yang L, Cheng Z, Yu X, Han Z, Liu F, Sun Q, Han X, Yu J, et al. BCL6B hypermethylation predicts metastasis and poor prognosis in early-stage hepatocellular carcinoma after thermal ablation. J Cancer Res Ther. 2021;17(3):644–51.
6. Gu Y, Li A, Sun H, Li X, Zha H, Zhao J, Xie J, Zeng Z, Zhou L. BCL6B suppresses proliferation and migration of colorectal carcinoma cells through inhibition of the PI3K/AKT signaling pathway. Int J Mol Med. 2018;41(5):2660–8.
7. Hu S, Cao B, Zhang M, Linghu E, Zhan Q, Brock MV, Herman JG, Mao G, Guo M. Epigenetic silencing BCL6B induced colorectal cancer proliferation and metastasis by inhibiting P53 signaling. Am J Cancer Res. 2015;5(2):651–62.
8. Ying J, Srivastava G, Hsieh WS, Gao Z, Murray P, Liao SK, Ambinder R, Tao Q. The stress-responsive gene GADD45G is a functional tumor suppressor, with its response to environmental stresses frequently disrupted epigenetically in multiple tumors. Clin Cancer Res. 2005;11(18):6442–9.
9. Tanaka M, Nakamura S, Sakaue T, Yamamoto T, Maekawa M, Nishinaka A, Yasuda H, Yunoki K, Sato Y, Sawa M, et al. BCL6B Contributes to Ocular Vascular Diseases via Notch Signal Silencing. Arterioscler Thromb Vasc Biol. 2023;43(6):927–42.
10. Ohnuki H, Inoue H, Takemori N, Nakayama H, Sakaue T, Fukuda S, Miwa D, Nishiwaki E, Hatano M, Tokuhisa T, et al. BAZF, a novel component of cullin3-based E3 ligase complex, mediates VEGFR and Notch cross-signaling in angiogenesis. Blood. 2012;119(11):2688–98.
11. Takahashi K, Tanabe K, Ohnuki M, Narita M, Ichisaka T, Tomoda K, Yamanaka S. Induction of pluripotent stem cells from adult human fibroblasts by defined factors. Cell. 2007;131(5):861–72.
12. Joung J, Ma S, Tay T, Geiger-Schuller KR, Kirchgatterer PC, Verdine VK, Guo B, Arias-Garcia MA, Allen WE, Singh A, et al. A transcription factor atlas of directed differentiation. Cell. 2023;186(1):209–229e226.
13. Clevers H. Modeling Development and Disease with Organoids. Cell. 2016;165(7):1586–97.
14. Tang XY, Wu S, Wang D, Chu C, Hong Y, Tao M, Hu H, Xu M, Guo X, Liu Y. Human organoids in basic research and clinical applications. Signal Transduct Target Ther. 2022;7(1):168.
15. Patsch C, Challet-Meylan L, Thoma EC, Urich E, Heckel T, O'Sullivan JF, Grainger SJ, Kapp FG, Sun L, Christensen K, et al. Generation of vascular endothelial and smooth muscle cells from human

pluripotent stem cells. Nat Cell Biol. 2015;17(8):994–1003.

16. Wimmer RA, Leopoldi A, Aichinger M, Kerjaschki D, Penninger JM. Generation of blood vessel organoids from human pluripotent stem cells. Nat Protoc. 2019;14(11):3082–100.
17. Moffat J, Grueneberg DA, Yang X, Kim SY, Kloepfer AM, Hinkle G, Piqani B, Eisenhaure TM, Luo B, Grenier JK, et al. A lentiviral RNAi library for human and mouse genes applied to an arrayed viral high-content screen. Cell. 2006;124(6):1283–98.
18. Kodaka Y, Asakura Y, Asakura A. Spin infection enables efficient gene delivery to muscle stem cells. Biotechniques. 2017;63(2):72–6.
19. Apte RS, Chen DS, Ferrara N. VEGF in Signaling and Disease: Beyond Discovery and Development. Cell. 2019;176(6):1248–64.
20. Qiu J, Hirschi KK. Endothelial Cell Development and Its Application to Regenerative Medicine. Circ Res. 2019;125(4):489–501.
21. Oh SY, Kim JY, Park C. The ETS Factor, ETV2: a Master Regulator for Vascular Endothelial Cell Development. Mol Cells. 2015;38(12):1029–36.
22. Kataoka H, Hayashi M, Nakagawa R, Tanaka Y, Izumi N, Nishikawa S, Jakt ML, Tarui H, Nishikawa S. Etv2/ER71 induces vascular mesoderm from Flk1 + PDGFRα + primitive mesoderm. Blood. 2011;118(26):6975–86.
23. Wang K, Lin RZ, Hong X, Ng AH, Lee CN, Neumeyer J, Wang G, Wang X, Ma M, Pu WT, et al. Robust differentiation of human pluripotent stem cells into endothelial cells via temporal modulation of ETV2 with modified mRNA. Sci Adv. 2020;6(30):eaba7606.
24. Reed DM, Foldes G, Harding SE, Mitchell JA. Stem cell-derived endothelial cells for cardiovascular disease: a therapeutic perspective. Br J Clin Pharmacol. 2013;75(4):897–906.
25. Wilson HK, Canfield SG, Shusta EV, Palecek SP. Concise review: tissue-specific microvascular endothelial cells derived from human pluripotent stem cells. Stem Cells. 2014;32(12):3037–45.
26. Cochrane A, Kelaini S, Tsifaki M, Bojdo J, Vilà-González M, Drehmer D, Caines R, Magee C, Eleftheriadou M, Hu Y, et al. Quaking Is a Key Regulator of Endothelial Cell Differentiation, Neovascularization, and Angiogenesis. Stem Cells. 2017;35(4):952–66.
27. Fernandez-Alonso R, Martin-Lopez M, Gonzalez-Cano L, Garcia S, Castrillo F, Diez-Prieto I, Fernandez-Corona A, Lorenzo-Marcos ME, Li X, Claesson-Welsh L, et al. p73 is required for endothelial cell differentiation, migration and the formation of vascular networks regulating VEGF and TGFβ signaling. Cell Death Differ. 2015;22(8):1287–99.
28. Olmer R, Engels L, Usman A, Menke S, Malik MNH, Pessler F, Göhring G, Bornhorst D, Bolten S, Abdelilah-Seyfried S, et al. Differentiation of Human Pluripotent Stem Cells into Functional Endothelial Cells in Scalable Suspension Culture. Stem Cell Rep. 2018;10(5):1657–72.
29. Rosowski S, Remmert C, Marder M, Akishiba M, Bushe J, Feuchtinger A, Platen A, Ussar S, Theis F, Wiedenmann S, et al. Single-cell characterization of neovascularization using hiPSC-derived endothelial cells in a 3D microenvironment. Stem Cell Rep. 2023;18(10):1972–86.

30. Tiemeier GL, Wang G, Dumas SJ, Sol W, Avramut MC, Karakach T, Orlova VV, van den Berg CW, Mummery CL, Carmeliet P, et al. Closing the Mitochondrial Permeability Transition Pore in hiPSC-Derived Endothelial Cells Induces Glycocalyx Formation and Functional Maturation. Stem Cell Rep. 2019;13(5):803–16.
31. Quan Y, Shan X, Hu M, Jin P, Ma J, Fan J, Yang J, Zhang H, Fan X, Gong Y, et al. YAP inhibition promotes endothelial cell differentiation from pluripotent stem cell through EC master transcription factor FLI1. J Mol Cell Cardiol. 2022;163:81–96.
32. James D, Nam HS, Seandel M, Nolan D, Janovitz T, Tomishima M, Studer L, Lee G, Lyden D, Benezra R, et al. Expansion and maintenance of human embryonic stem cell-derived endothelial cells by TGFbeta inhibition is Id1 dependent. Nat Biotechnol. 2010;28(2):161–6.
33. Trimm E, Red-Horse K. Vascular endothelial cell development and diversity. Nat Rev Cardiol. 2023;20(3):197–210.
34. Tombor LS, John D, Glaser SF, Luxán G, Forte E, Furtado M, Rosenthal N, Baumgarten N, Schulz MH, Wittig J, et al. Single cell sequencing reveals endothelial plasticity with transient mesenchymal activation after myocardial infarction. Nat Commun. 2021;12(1):681.
35. Nitzsche A, Poittevin M, Benarab A, Bonnin P, Faraco G, Uchida H, Favre J, Garcia-Bonilla L, Garcia MCL, Léger PL, et al. Endothelial S1P(1) Signaling Counteracts Infarct Expansion in Ischemic Stroke. Circ Res. 2021;128(3):363–82.

# Figures

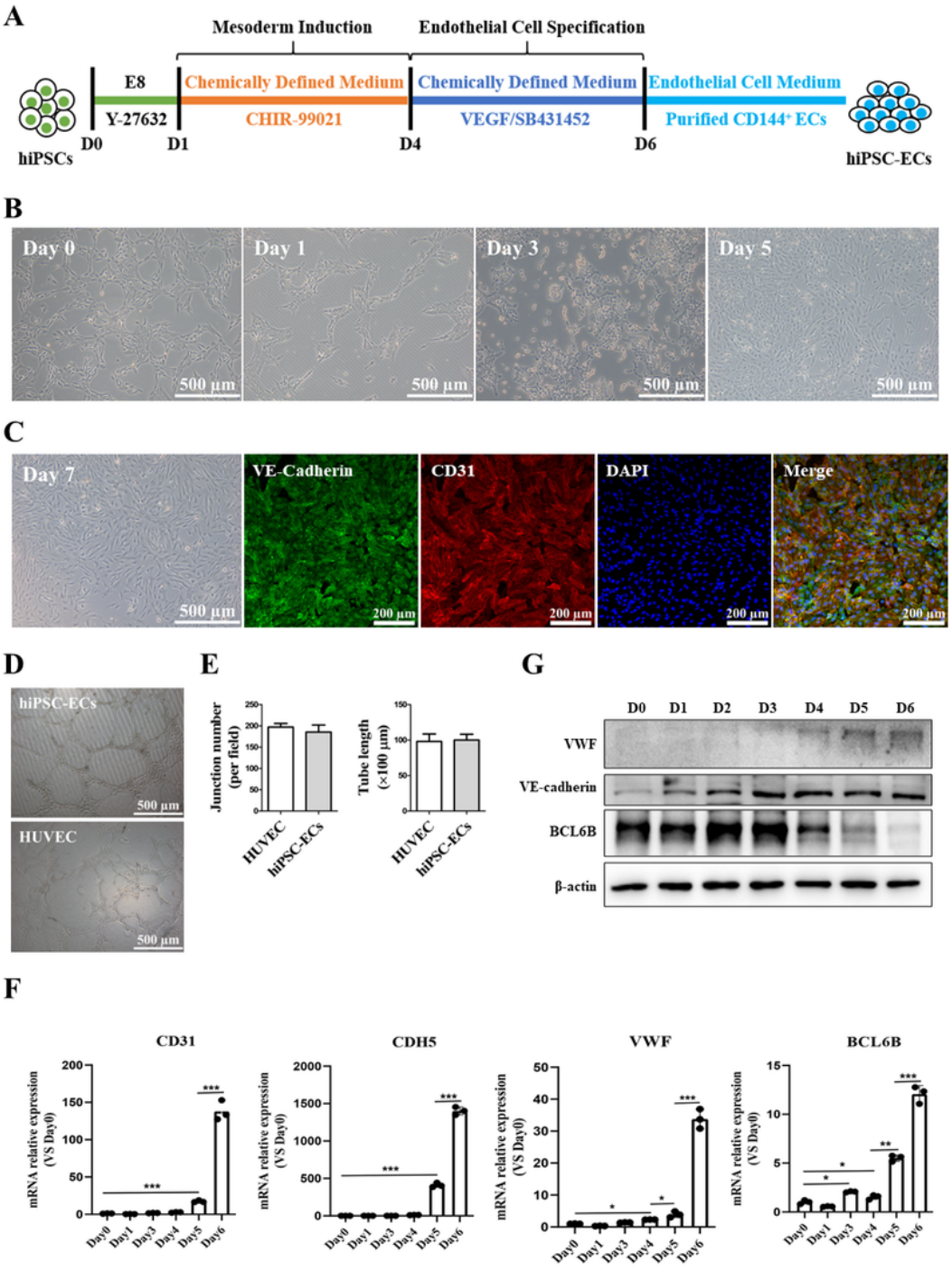


## Figure 1

### Generation and characterization of hiPSC-derived ECs

(A) Schematic illustration outlining the strategy for EC differentiation from hiPSCs. The differentiation of hiPSCs into ECs involved two stages: mesoderm induction and EC specification, with the entire process typically taking 6 days.

(B) Brightfield images depicting the cell morphology at different time points during EC differentiation.

(C) Brightfield image showing purified ECs at D7, along with confocal immunofluorescence images highlighting EC markers VE-Cadherin (green) and CD31 (red) with DAPI (blue).

(D) Brightfield images displaying tube-like structures formed by hiPSC-ECs and HUVEC.

(E) Quantitative analysis of junction number and tube length.

(F) mRNA expression of EC markers (*VWF*, *CDH5*, *CD31*) and *BCL6B* during EC differentiation.

(G) Protein levels of VWF, VE-Cadherin and BCL6B throughout EC differentiation from D0 to D6, as determined by western blot. Full-length blots were presented in Supplementary Figure 1.

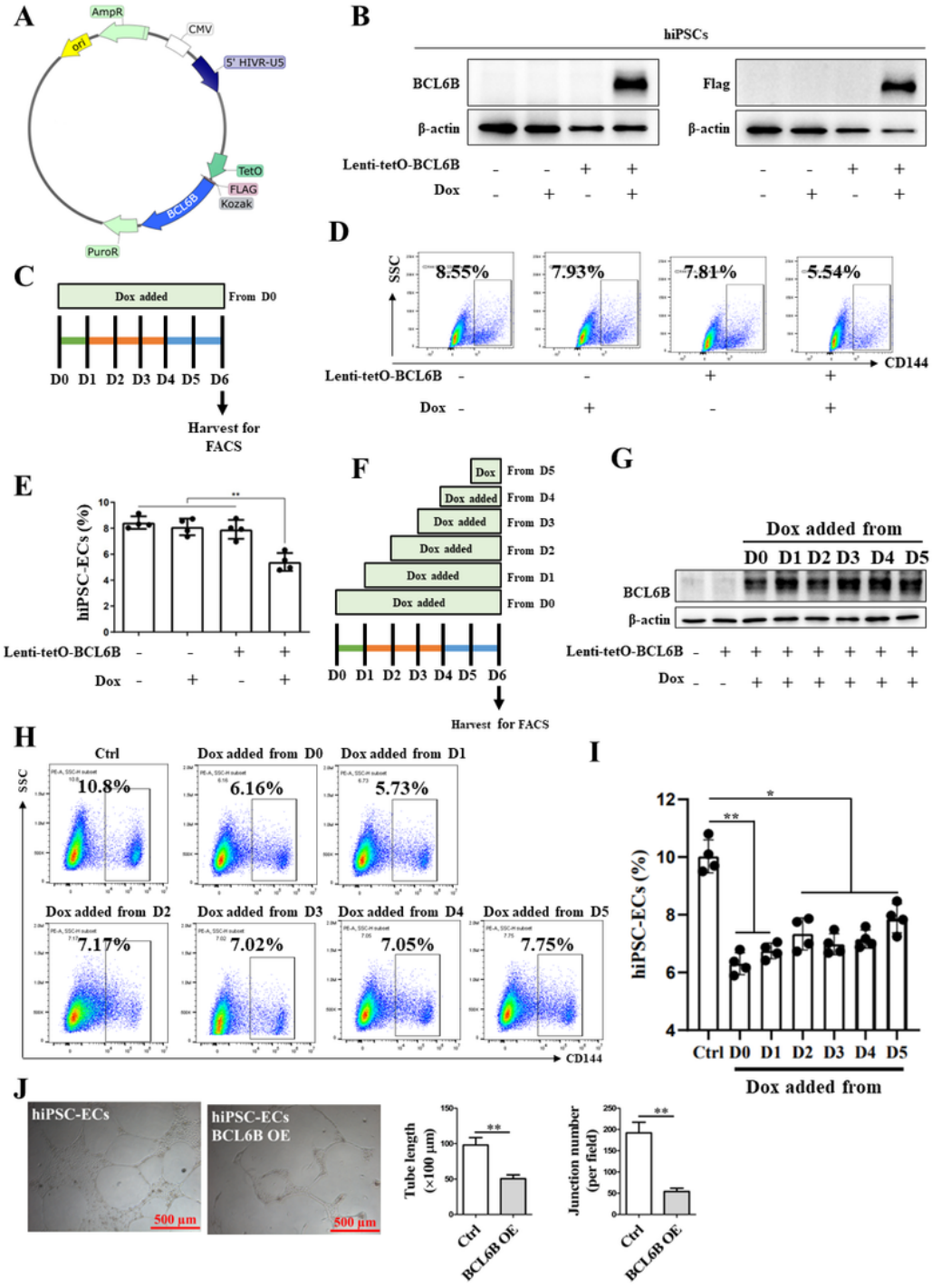


## Figure 2

### BCL6B overexpression suppressed ECs differentiation from hiPSCs

(A) Schematic illustration of the doxycycline-induced BCL6B overexpression vector using the tetO-on system.

(B) Verification of doxycycline-induced BCL6B protein expression in the established inducible BCL6B-overexpression hiPSC line (BCL6B OE). Full-length blots were presented in Supplementary Figure 2.

(C) Schematic illustration of doxycycline addition to induce BCL6B overexpression.

(D) Representative flow cytometry results of $CD144^+$ cells in hiPSC-ECs from different groups.

(E) Statistical analysis of the $CD144^+$ cells in hiPSC-ECs from different groups. **, $P<0.01$.

(F) Schematic illustration of doxycycline addition at different time points.

(G) BCL6B protein expression in D6 ECs derived from BCL6B OE hiPSC started to be treated with doxycycline at different time points. Full-length blots were presented in Supplementary Figure 3.

(H) Representative flow cytometry results of $CD144^+$ cells in iPSC-ECs from different groups.

(I) Statistical analysis of the $CD144^+$ cells in hiPSC-ECs from different groups. *, $P<0.05$; **, $P<0.01$.

(J) Representative brightfield images of tube-like structures formed by hiPSC-ECs and BCL6B OE hiPSC-ECs (left panel), and quantitative analysis of tube length and junction number (right panel). OE, overexpression. **, $P<0.01$.

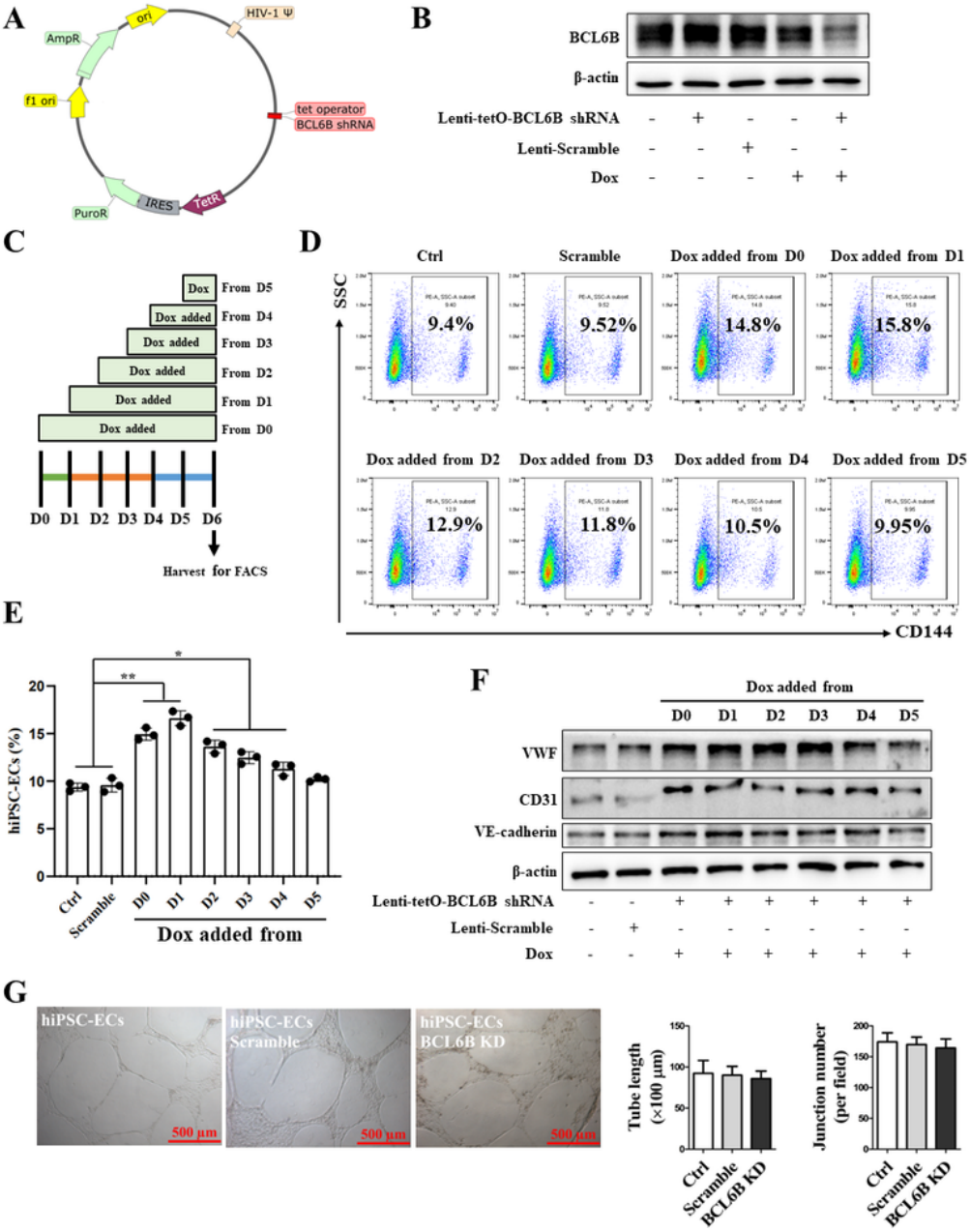


## Figure 3

### Downregulation of BCL6B improved ECs differentiation from hiPSCs

(A) Schematic illustration of the doxycycline-induced BCL6B shRNA vector using the tetO-on system.

(B) Verification of doxycycline-induced BCL6B protein knock-down in the established inducible BCL6B-knock down hiPSC line (BCL6B KD). Full-length blots were presented in Supplementary Figure 4.

(C) Schematic illustration of doxycycline addition to induce BCL6B knockdown.

(D) Representative flow cytometry results of $CD144^+$ cells in hiPSC-ECs from different groups.

(E) Statistical analysis of the $CD144^+$ cells in hiPSC-ECs from different groups. *, $P<0.05$; **, $P<0.01$.

(F) Protein levels of VWF, VE-cadherin and CD31 in D6 ECs derived from BCL6B KD hiPSC started to be treated with doxycycline at different time points. Full-length blots were presented in Supplementary Figure 5.

(G) Representative brightfield images of tube-like structures formed by hiPSC-EC and BCL6B KD hiPSC-ECs (left panel), and quantitative analysis of tube length and junction number (right panel).

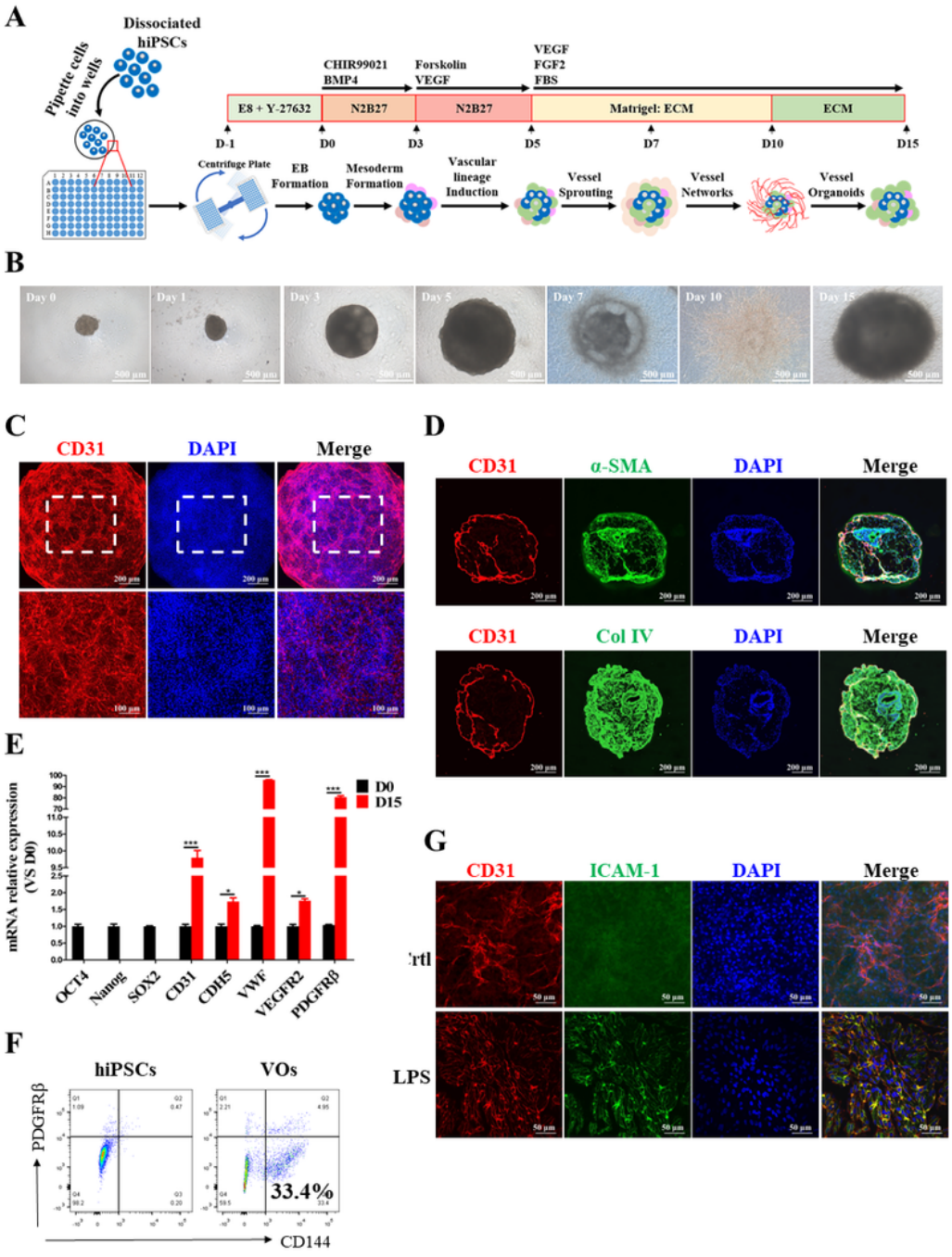


## Figure 4

### Generation and characterization of blood VOs

(A) A schematic diagram illustrating the protocol used to generate VOs from hiPSCs.

(B) Brightfield images depicting the development of VOs over a 15-day differentiation period.

(C) Confocal imaging of CD31 in D15 VOs.

(D) Immunostaining of α-SMA, Col and CD31 in D15 VOs. α-SMA, alpha- smooth muscle cell actin; Col , Collagen IV.

(E) mRNA expression of stem markers (*Nanog*, *OCT4*, *SOX2*) and vessel markers (*VWF*, *CDH5*, *CD31*, *VEGFR2* and *PDGFRβ*) in D15 VOs (n=10) compared to D0. Data normalized to *GAPDH* expression.

(F) Flow cytometry analysis of $PDGFR\beta^+$ and $CD144^+$ cells in D15 VOs.

(G) Immunostaining of ICAM-1 expression in D15 VOs after treatment of LPS (2 μg/mL) for 24 hours.

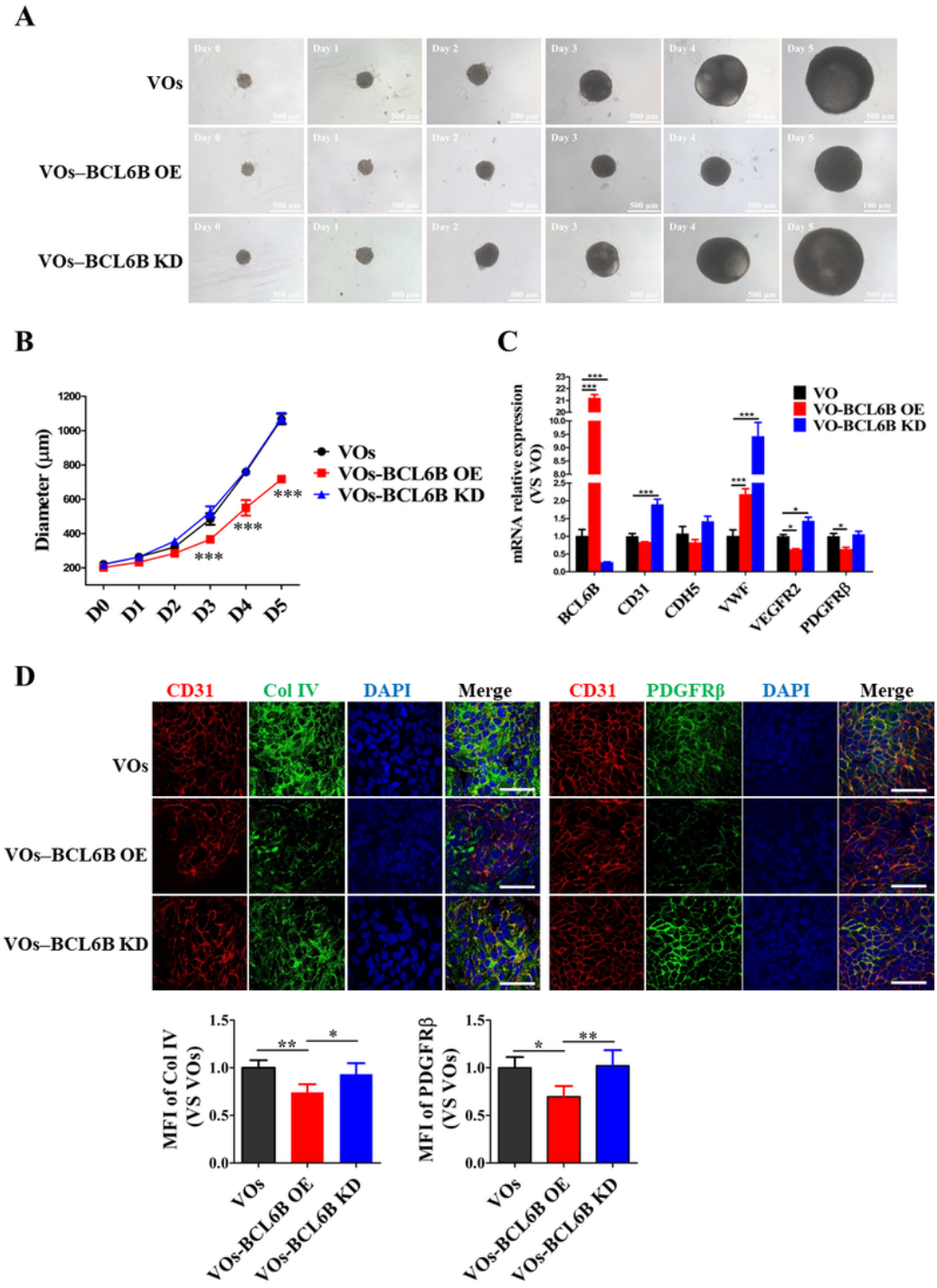


## Figure 5

### Overexpression of BCL6B impaired VOs development

(A) Brightfield images illustrating the development of VOs from hiPSCs with or without BCL6B gene manipulation over a 6-day differentiation period.

(B) Statistical analysis of the diameter of VOs derived from control, BCL6B OE, and BCL6B KD hiPSCs. N=16; ***, *P*<0.001.

(C) mRNA expression of vessel markers (*VWF*, *CDH5*, *CD31*, *VEGFR2* and *PDGFRβ*) and *BCL6B* in D15 VOs (n=10). Data normalized to *GAPDH* expression.

(D) Immunostaining and quantification of PDGFRβ and Col in D15 VOs. Col , Collagen IV. *, *P*<0.05; **, *P*<0.01.

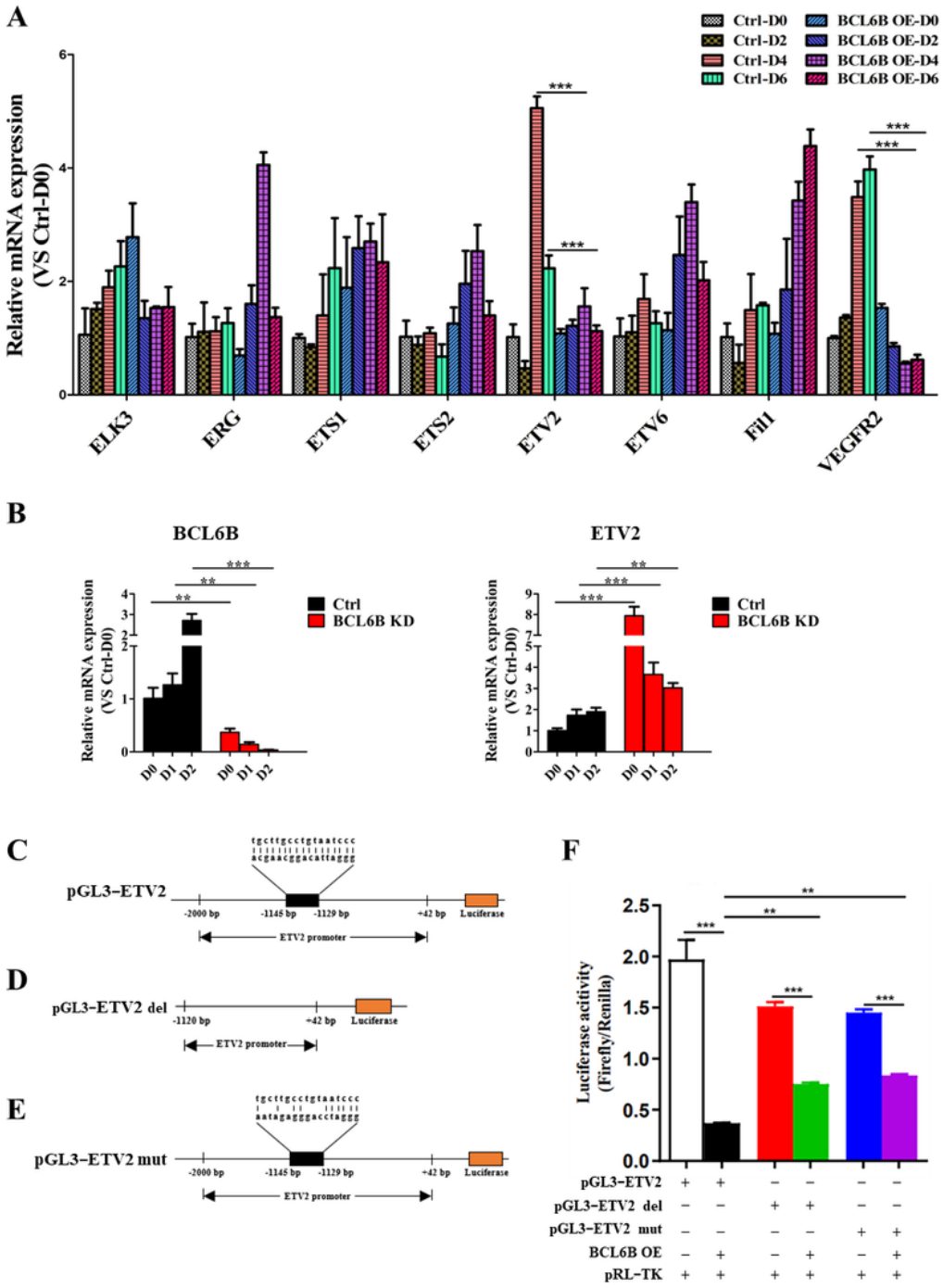


## Figure 6

## BCL6B inhibited ETV2 transcription

(A) mRNA expression of *ETS1*, *ETS2*, *ELK3*, *ERG*, *ETV2*, *ETV6*, *Fil1* and *VEGFR2* during EC differentiation from control or BCL6B OE hiPSCs. Data normalized to *GAPDH* expression.

(B) mRNA expression of *BCL6B* (left panel) and *ETV2* ((right panel)) at early stage during EC differentiation from control or BCL6B KD hiPSCs. Data normalized to *GAPDH* expression. **, $P<0.01$; ***, $P<0.001$.

(C-E) Schematic illustration of three luciferase reporter vectors carrying the full-length (C), truncated (D) or mutated (E) ETV2 gene promoters.

(F) Luciferase activity in 293T cells after transfection with luciferase reporter vectors, with or without the BCL6B overexpression vector for 24 hours. The renilla luciferase vector (pRL-TK) was co-transfected as a control. **, $P<0.01$; ***, $P<0.001$.

## Supplementary Files

This is a list of supplementary files associated with this preprint. Click to download.

- SupplementaryFigure.pdf